

CHAPTER III

X - RAY DIFFRACTION STUDY

3.1 The Structure Of Perovskite -Type Ferroelectrics

The perovskite - type ferroelectrics with general composition ABO_3 (Ba TiO_3) have the cubic unit cell as shown fig (3.1). The space group is $O'_h - P_m 3m$. Placing the origin of an A ion the atomic co-ordinates are as follows :-

A ---- at - 0, 0, 0;

B ---- at - $\frac{1}{2}$, $\frac{1}{2}$, $\frac{1}{2}$;

3O ---- at - $\frac{1}{2}$, $\frac{1}{2}$, 0; 0, $\frac{1}{2}$, $\frac{1}{2}$; $\frac{1}{2}$, 0, $\frac{1}{2}$;

With decreasing temperature the crystal transform first into tetragonal, polarised phase with symmetry $C_{4v} - P4mm$. The ions are displaced from their original high symmetry position along the polar axis Z. Again taking A at the origin the co-ordinates are :-

A ---- at - 0, 0, 0;

B ---- at - $\frac{1}{2}$, $\frac{1}{2}$, $\frac{1}{2} + \delta Z_B$;

O_I ---- at - $\frac{1}{2}$, $\frac{1}{2}$, δZ_{OI} ;

2 O_{II} ---- at - $\frac{1}{2}$, 0, $\frac{1}{2} + \delta Z_{OII}$; 0, $\frac{1}{2}$, $\frac{1}{2} + \delta Z_{OII}$

Though the structure is very simple, it exceedingly difficult to determine the small displacements δz . Part of this difficulty is inherent in the well known phase problem in diffraction analysis and in the existence of centre of symmetry in the undistorted structure. Considerable difficulties arise also from the thermal oscillation parameters. The determination of oxygen parameters with X-rays is particularly difficult in the presence of much heavier lattice constituents; neutron diffraction is a much more suitable tool in this case. Nevertheless the X-ray picture may provide an overall information about the tetragonal phase by providing the knowledge the values of lattice parameters 'a' and the ratio 'c/a.'

3.2 The structure of BaTiO₃ In The Tetragonal Phase :

The first detailed X-ray analysis of untwinned crystals was made by Kanzig (61) using rather unconventional method. Instead of deducting the displacements δz from the measured structure factors of a great number of reflections (h,k,l), Kanzig measured the change that high order (0, 0, 1) structure factors undergo when the crystal transforms from

the cubic phase into the tetragonal phase, the displacements δz were determined from these changes. It was assumed that O_{II} remains undisplaced and that δz_{Ti} and δz_{OI} have opposite signs. The parameters δz at room temperature were found to be

$$\delta z_{Ti} = 0.0114, \delta z_{OI} = -0.032$$

$$[\delta z_{OII} = 0 \text{ assumed}]$$

Using conventional methods, Evans (62) made thorough X-ray analysis of the tetragonal phase at room temperature without introducing the assumptions made in the earlier analysis, he deduced two structures which are in very good agreement with the observed intensities. The first solution is very close to Kanzig's result.

$$\delta z_{Ti} = 0.012, \delta z_{OI} = -0.026, \delta z_{OII} = 0$$

The second solution gave

$$\delta z_{Ti} = 0.015, \delta z_{OI} = -0.024, \delta z_{OII} = -0.020$$

A neutron analysis was accomplished by Frazer et al (63).

It led to the following parameters at room temperature.

$$\delta z_{Ti} = 0.014, \delta z_{OI} = -0.023, \delta z_{OII} = -0.014$$

If a purely ionic crystal is assumed these parameters correspond to an ionic displacement polarization of 17×10^{-6}

coul/cm² A neutron diffraction study of the orthorhombic phase has also been accomplished by Shirane et al (64).

3.3 Method Of Determination Of Parameters 'a' & 'c'

The method we have adopted is a graphical technique and was proposed by Hall & Deary. The method is described below.

The interplaner distance 'd' corresponding to any two planes with Miller indices h, k, l for a tetragonal unit cell is given by the relation.

$$d^2 = a^2 \left[h^2 + k^2 + l^2 \left(\frac{c}{a} \right)^2 \right]^{-1} \quad \text{---(3.1)}$$

Now the equation 3.1 has two unknowns, viz a and c/a to be determined knowing d values and corresponding h,k,l of the reflections in the XRD graph. The XRD graph provides knowledge about d values only and therefore intially h, k, l corresponding to the reflections and the parameter c/a is determined as below. Let d₁ and d₂ be the interplaner distances for any two plane sets with corresponding indices h₁, k₁, l₁ and h₂, k₂, l₂ respectively therefore,

$$d_1^2 = a^2 \left[h_1^2 + k_1^2 + l_1^2 \left(\frac{c}{a} \right)^2 \right]^{-1} \quad \text{---(3.2)}$$

$$d_2^2 = a^2 \left[h^2 + k^2 + l^2 \left(\frac{c}{a} \right)^2 \right]^{-1} \quad \text{---(3.3)}$$

Further taking logarithms on both the sides of equations 3.2 and 3.3 and subtracting eqn. 3.2 from eqn. 3.3 we find:-

$$2 \log d_2 - 2 \log d_1 = \log (h^2 + k^2 + l^2 (c/a)^2) - \log (h^2 + k^2 + l^2 (c/a)^2) \quad \dots(3.4)$$

The equation 3.4 is used for the graphical technique.

Initially the graph of $\log (h^2 + k^2 + l^2 (c/a)^2)$ for various values of c/a between 0.4 to 1.8 and for different values of h, k, l is plotted. The $\log (h^2 + k^2 + l^2 (c/a)^2)$ is plotted as abscissa, while c/a is the ordinate while selecting the scale on abscissa, the scale is selected as a negative logarithmic scale, such that

$$-\log (h^2 + k^2 + l^2 (c/a)^2)$$

is plotted automatically. Usually, 10cm equals one period of logarithm.

Now the values of $2 \log d$ are plotted on a transparent strip.

The scales selected for $\log (h^2 + k^2 + l^2 (c/a)^2)$ and $2 \log d$ are the same. Now the transparent strip is slid over the graph of $\log (h^2 + k^2 + l^2 (c/a)^2)$ and c/a , such that each $2 \log d$ value matches with some $\log (h^2 + k^2 + l^2 (c/a)^2)$

value. This will occur only for a c/a value, as seen from equ 3.4. The corresponding parameter c/a and h,k,l values are determined for every value of the interplaner distance. Using this information the parameters \bar{a} , a and c/a are calculated.

In the present investigation, we have tried to index the following planes and have determined the values of parameters a , \bar{a} and c/a . The planes selected are $(1,0,0)$, $(0,0,1)$, --

3.4 The Result And Discussion

In the present study an attempt has been made to determine lattice structure parameters of polycrystalline barium titanate ($BaTiO_3$) and solid solutions $BaFe_{x/2}Sb_{x/2}Ti_{(1-x)}O_3$ and $BaCr_{x/2}Sb_{x/2}Ti_{(1-x)}O_3$, for $x = 0.025, 0.05, 0.1, 0.2$ and 0.4 . Powder diffraction patterns are shown in fig 3.1, 3.2, 3.3, 3.4, 3.5, 3.6, 3.7, 3.8, 3.9. The prominent lines are indexed in these diffraction patterns. The results obtained from the analysis of these diffraction patterns as outlined in sec 3.3 are presented in table 3.1 and 3.2 along with earlier worker's data.

Fig 3.10 shows variation c/a as x for both the substitutions. The trends observed for Fe Sb substitution is opposite to that observed for Cr Sb substitution. The c/a

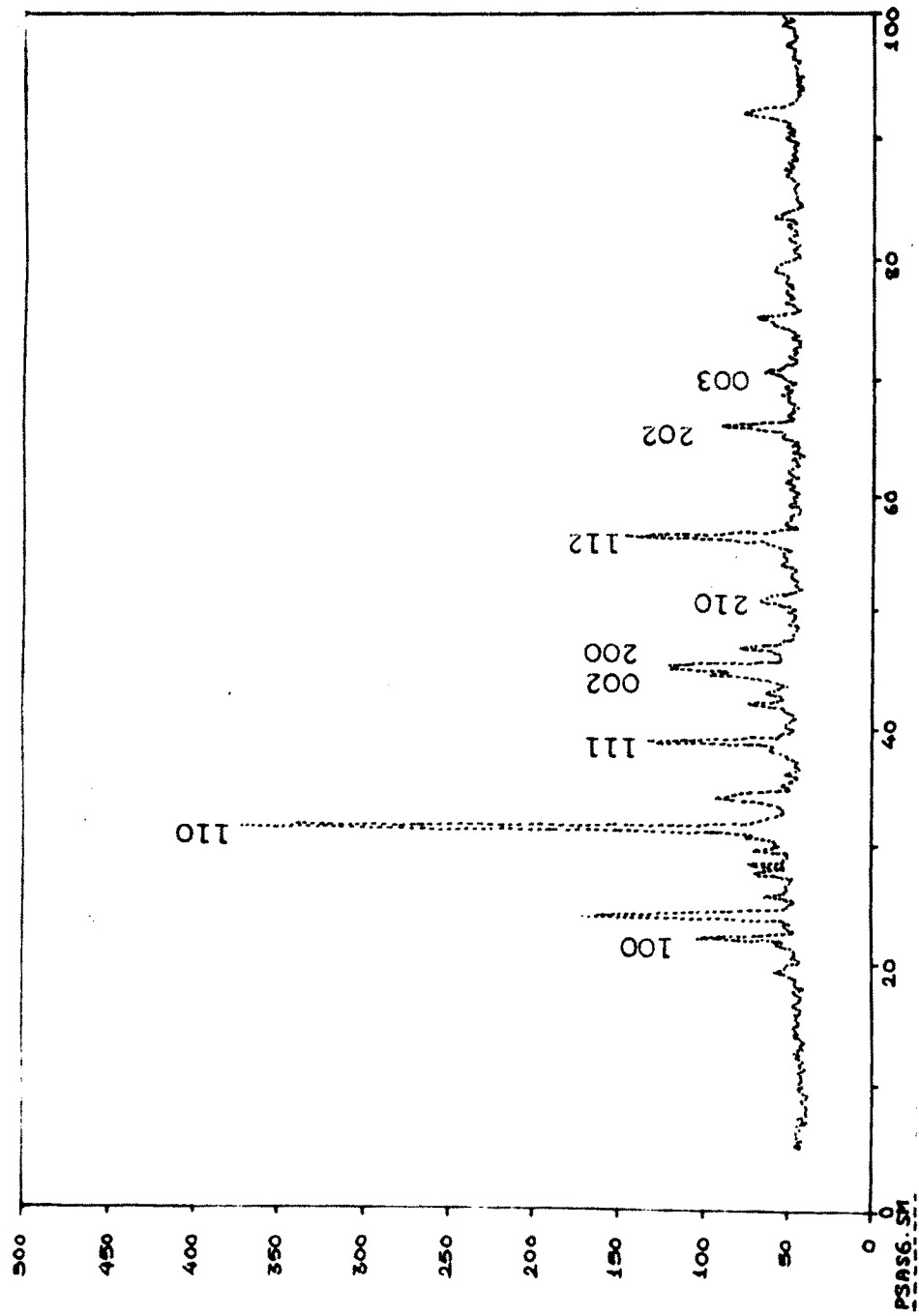


Fig.3.1 X-ray diffraction of BaTiO₃

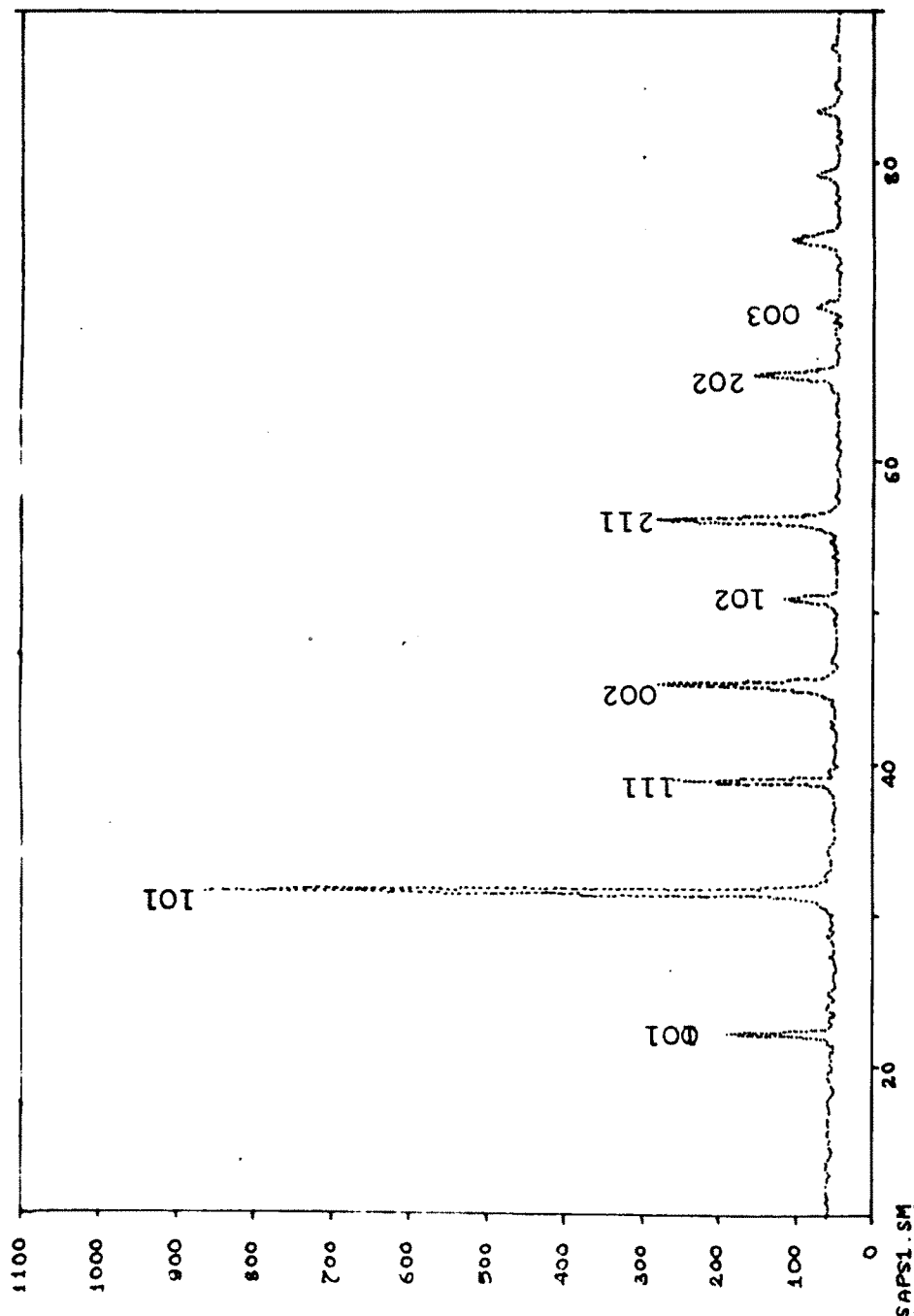


Fig.3.2 X-ray diffraction of BaFe_{0.0125}Sb_{0.0125}Ti_{0.975}O₃

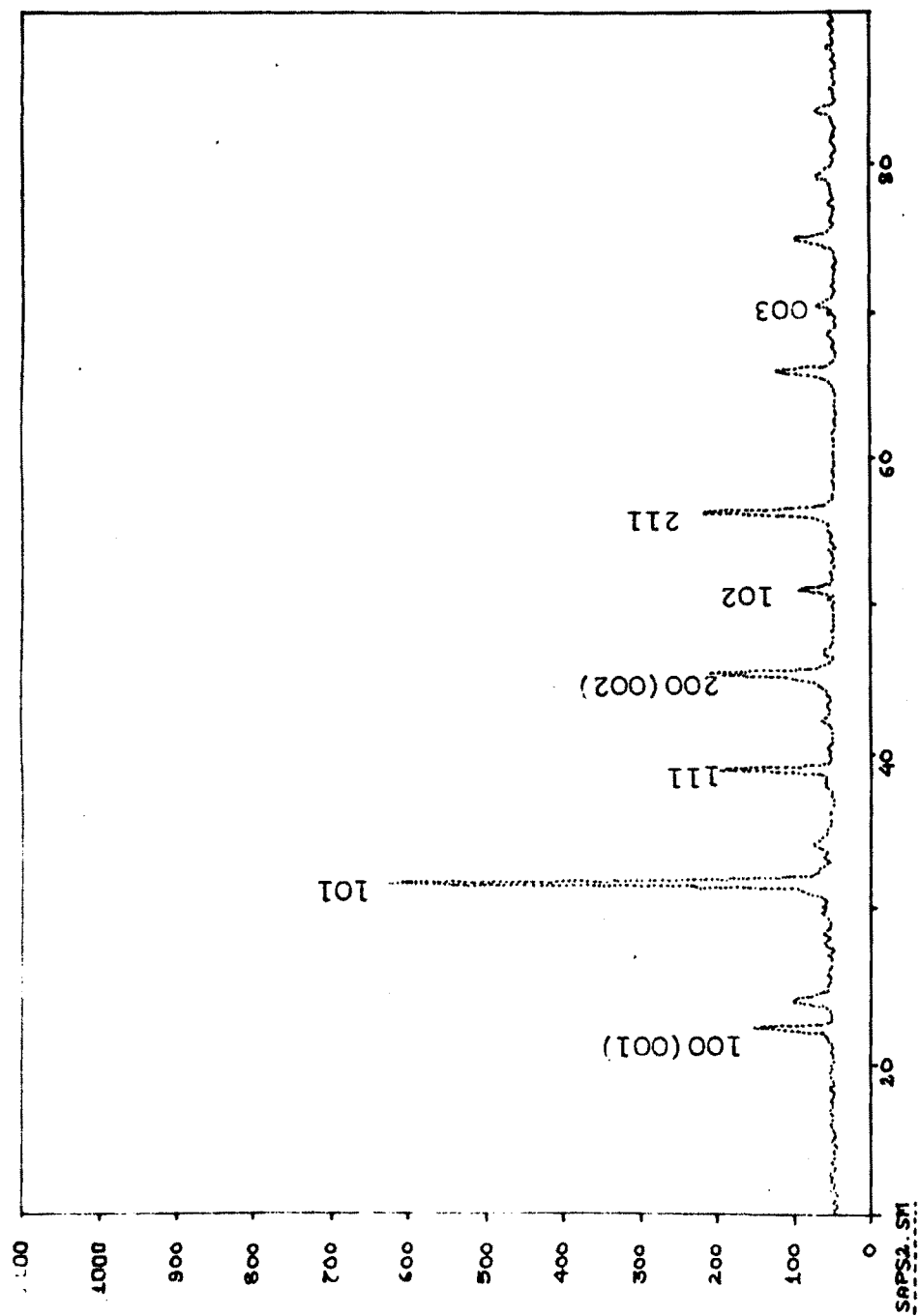


Fig.3.3 X-ray diffraction of BaFe_{0.025}Sb_{0.025}Ti_{0.95}O₃

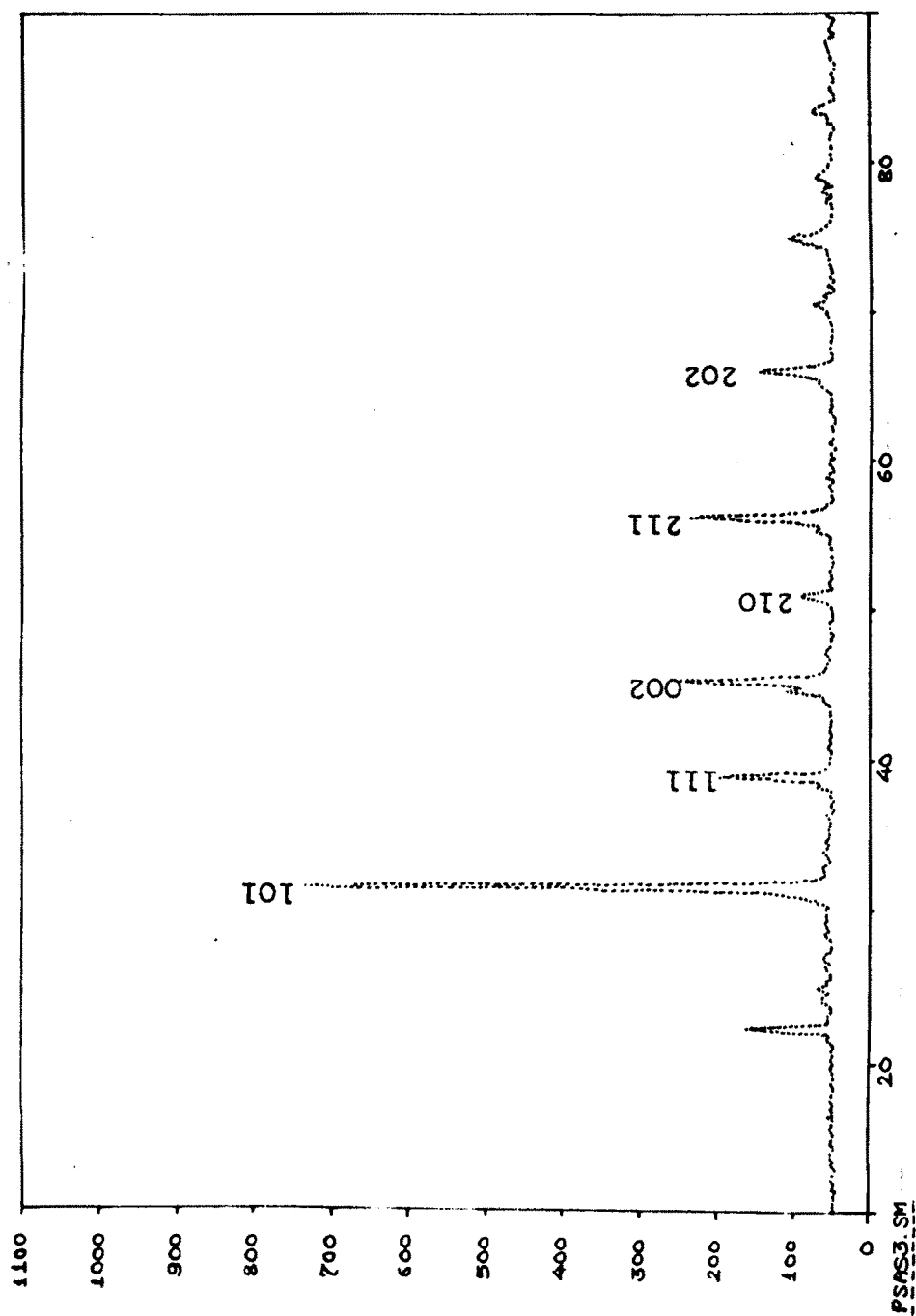


Fig.3.4 X-ray diffraction of $\text{BaFe}_{0.05}\text{Sb}_{0.05}\text{Ti}_{0.9}\text{O}_3$

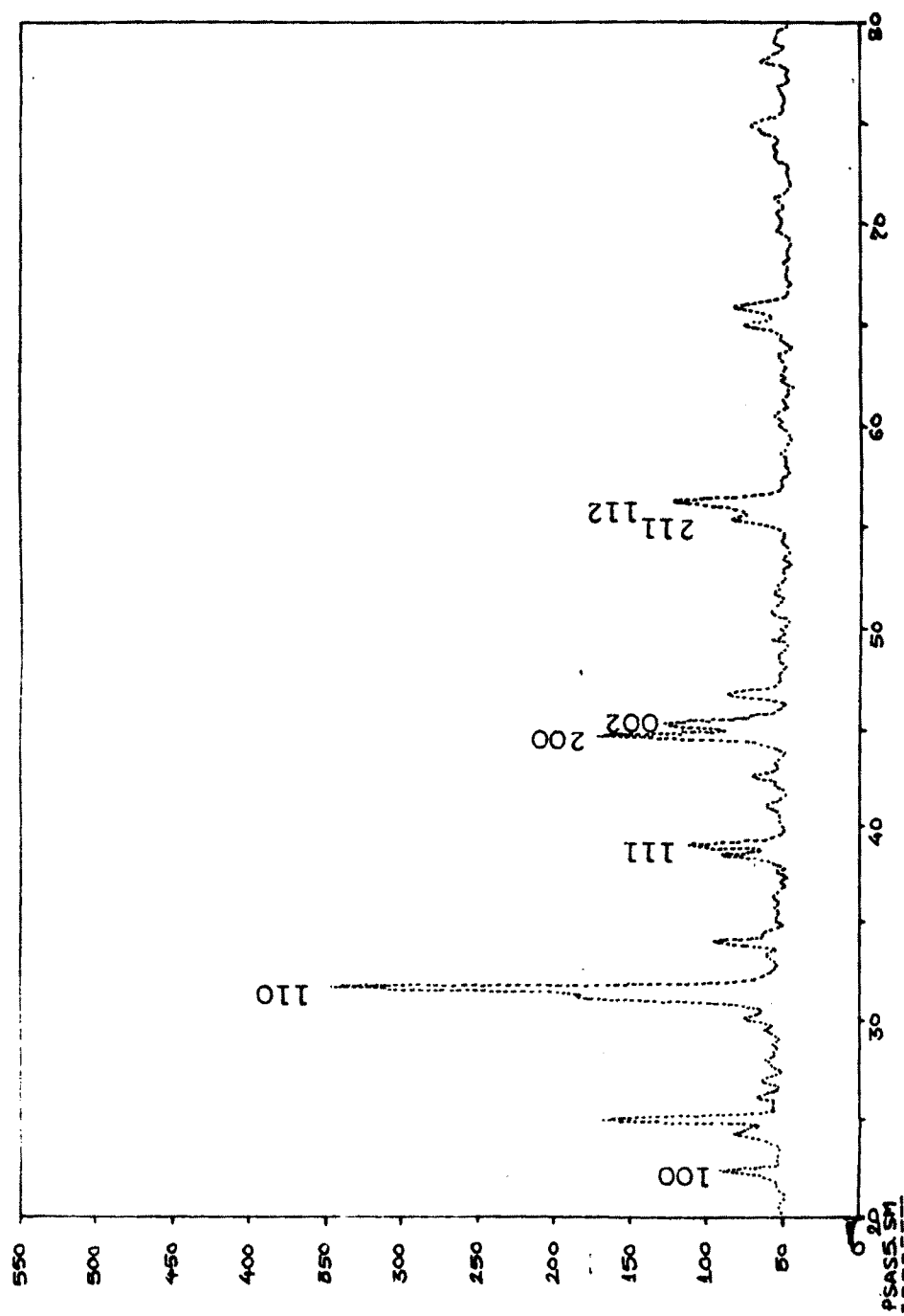


Fig.3.5 X-ray diffraction of $\text{BaFe}_{0.2}\text{Sb}_{0.2}\text{Ti}_{0.8}\text{O}_3$

P-1

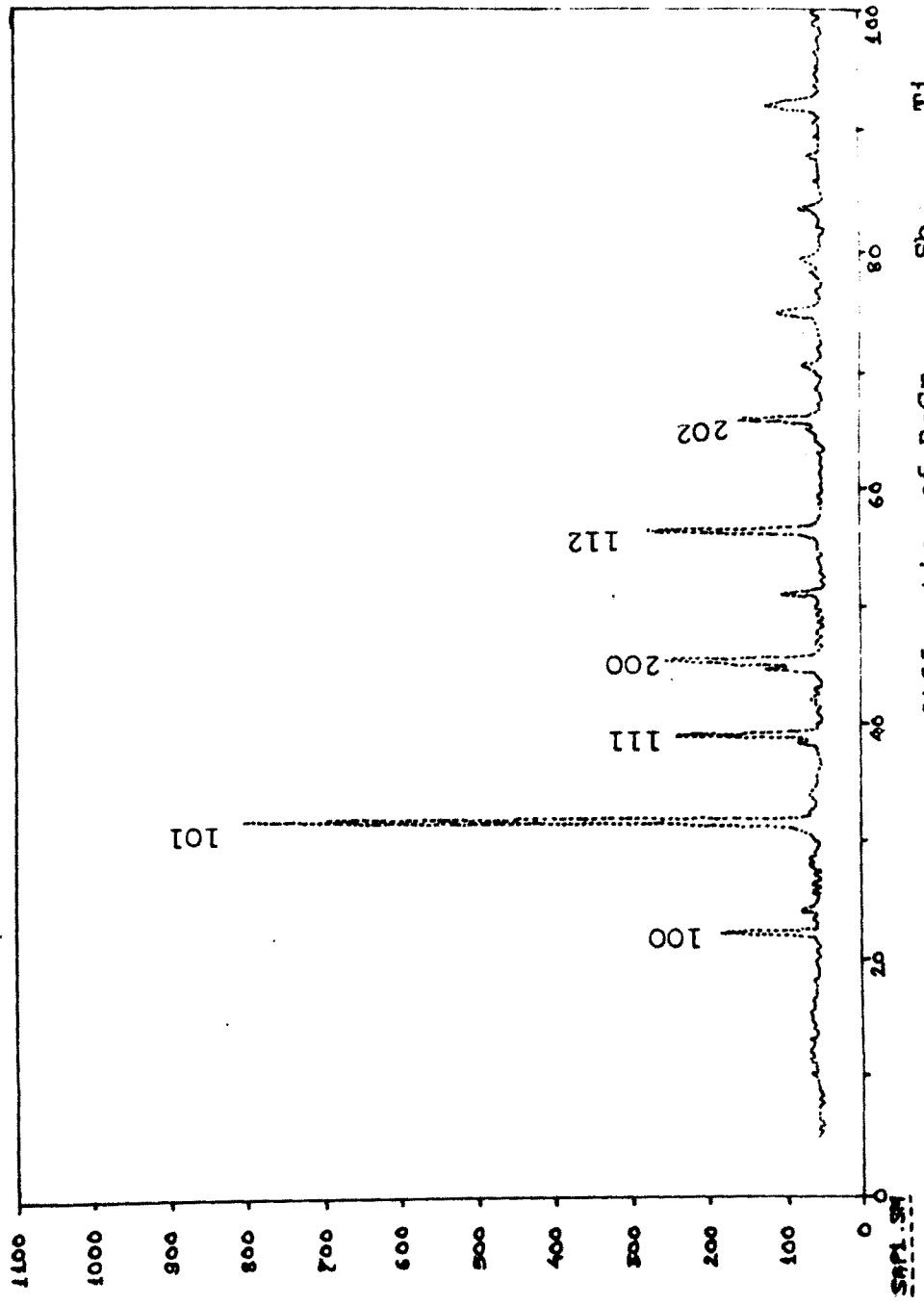


Fig.3.6 X-ray diffraction of BaCr_{0.0125}Sb_{0.0125}Tl_{0.975}O₃

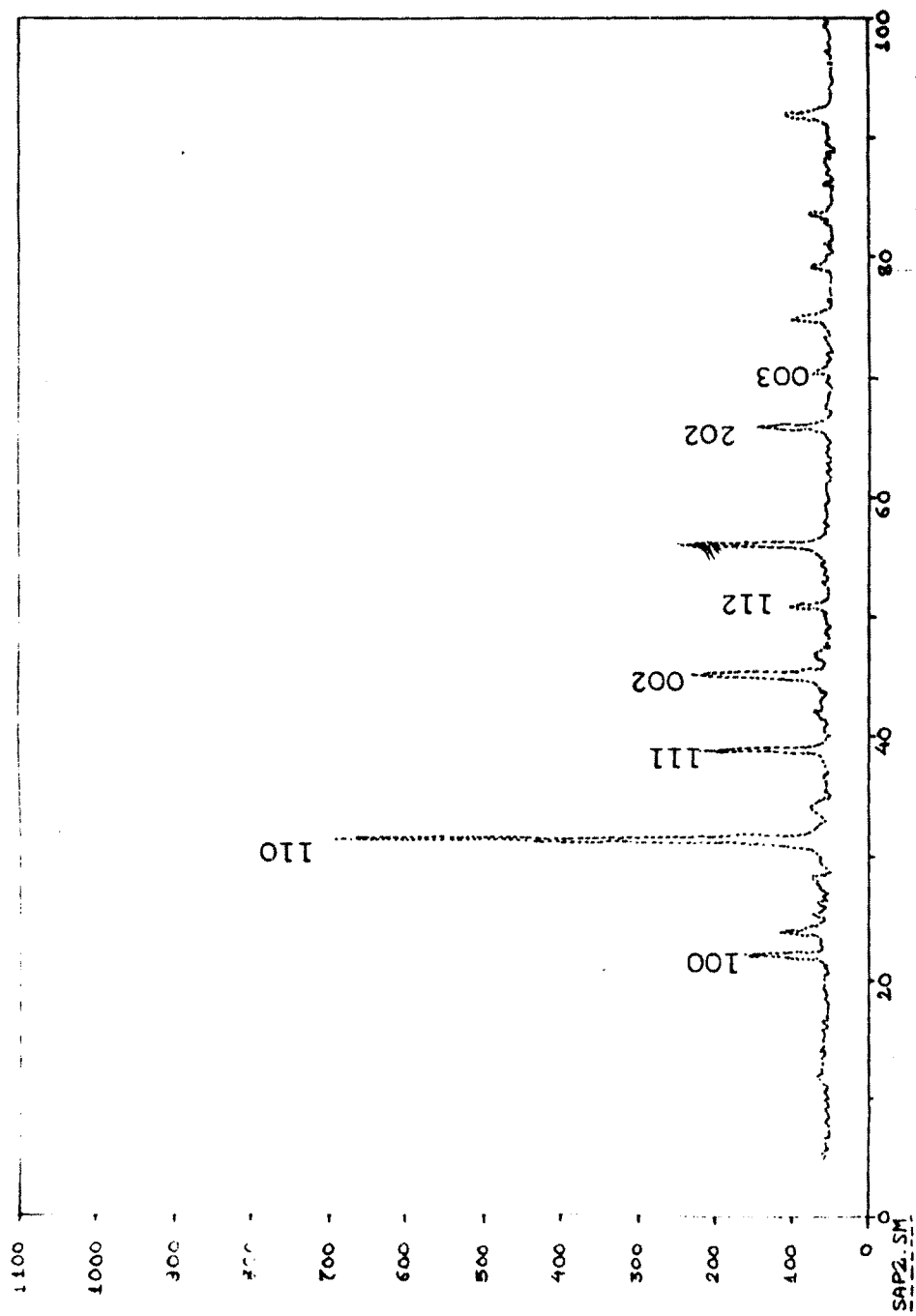


Fig.3.7 X-ray diffraction of $\text{BaCr}_{0.025}\text{Sb}_{0.025}\text{Ti}_{0.95}\text{O}_3$

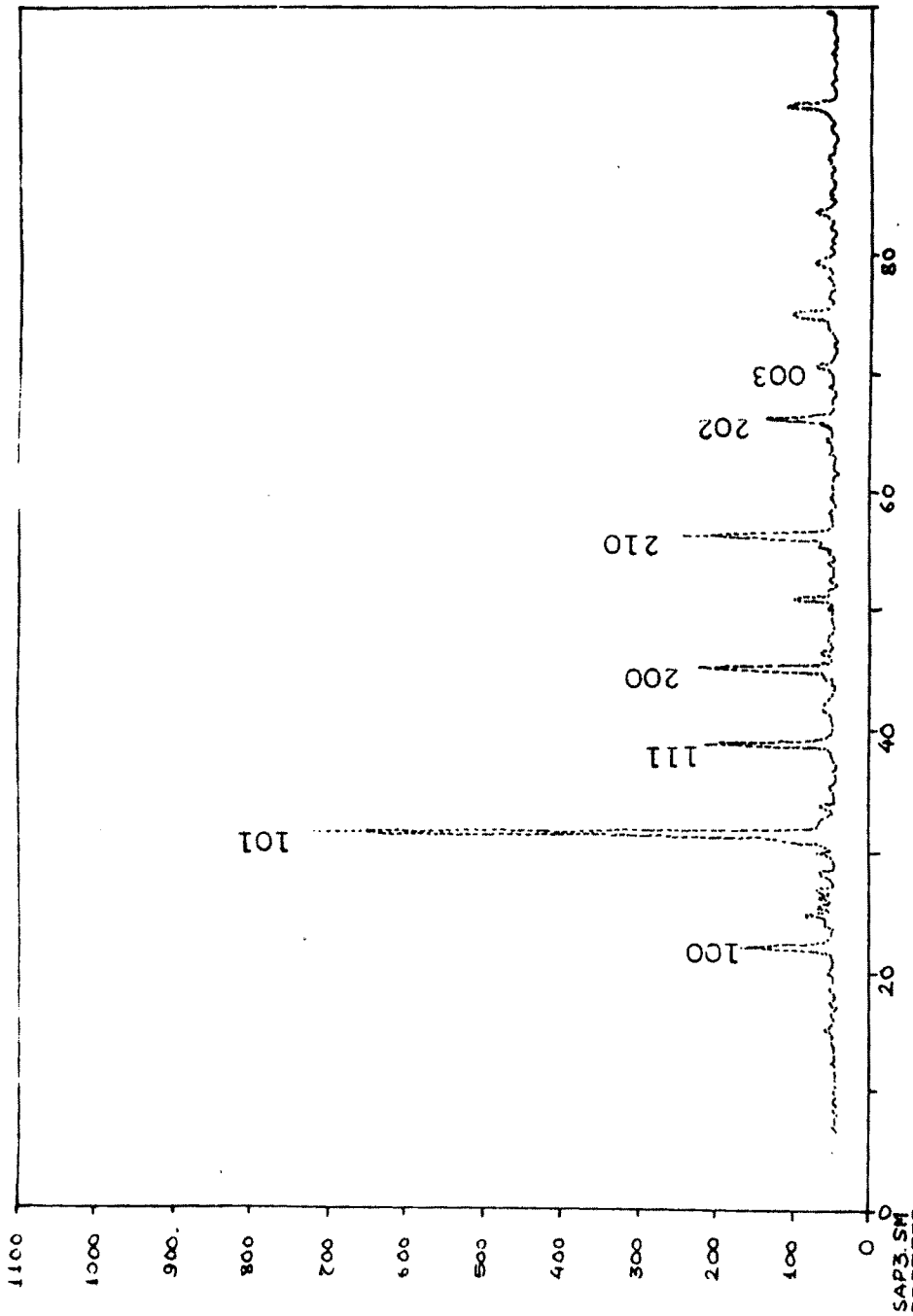


Fig.3.8 X-ray diffraction of $\text{BaCr}_{0.05}\text{Sb}_{0.05}\text{Ti}_{0.9}\text{O}_3$

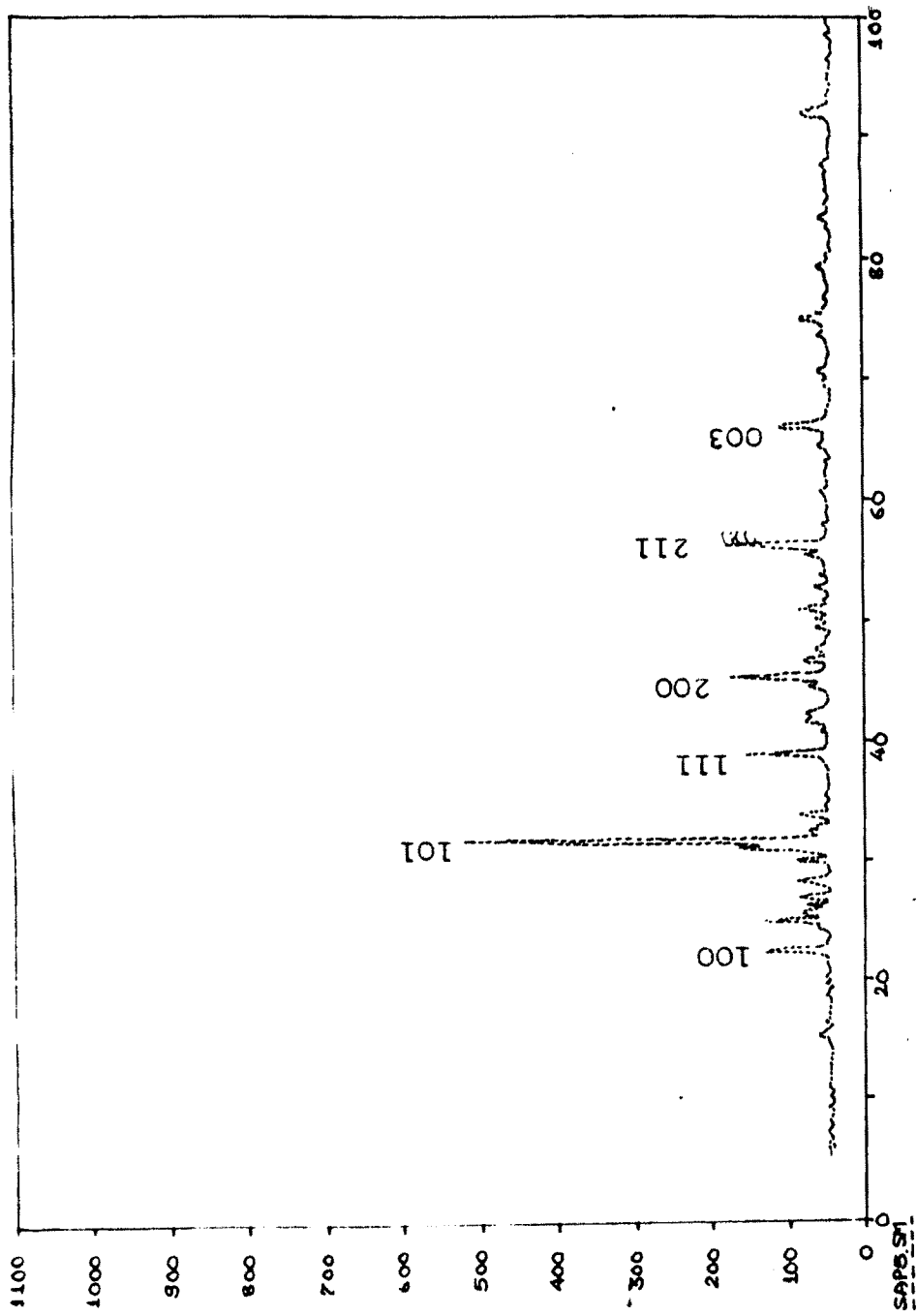


Fig.3.9 X-ray diffraction of $\text{BaCr}_{0.2}\text{Sb}_{0.2}\text{Ti}_{0.6}\text{O}_3$

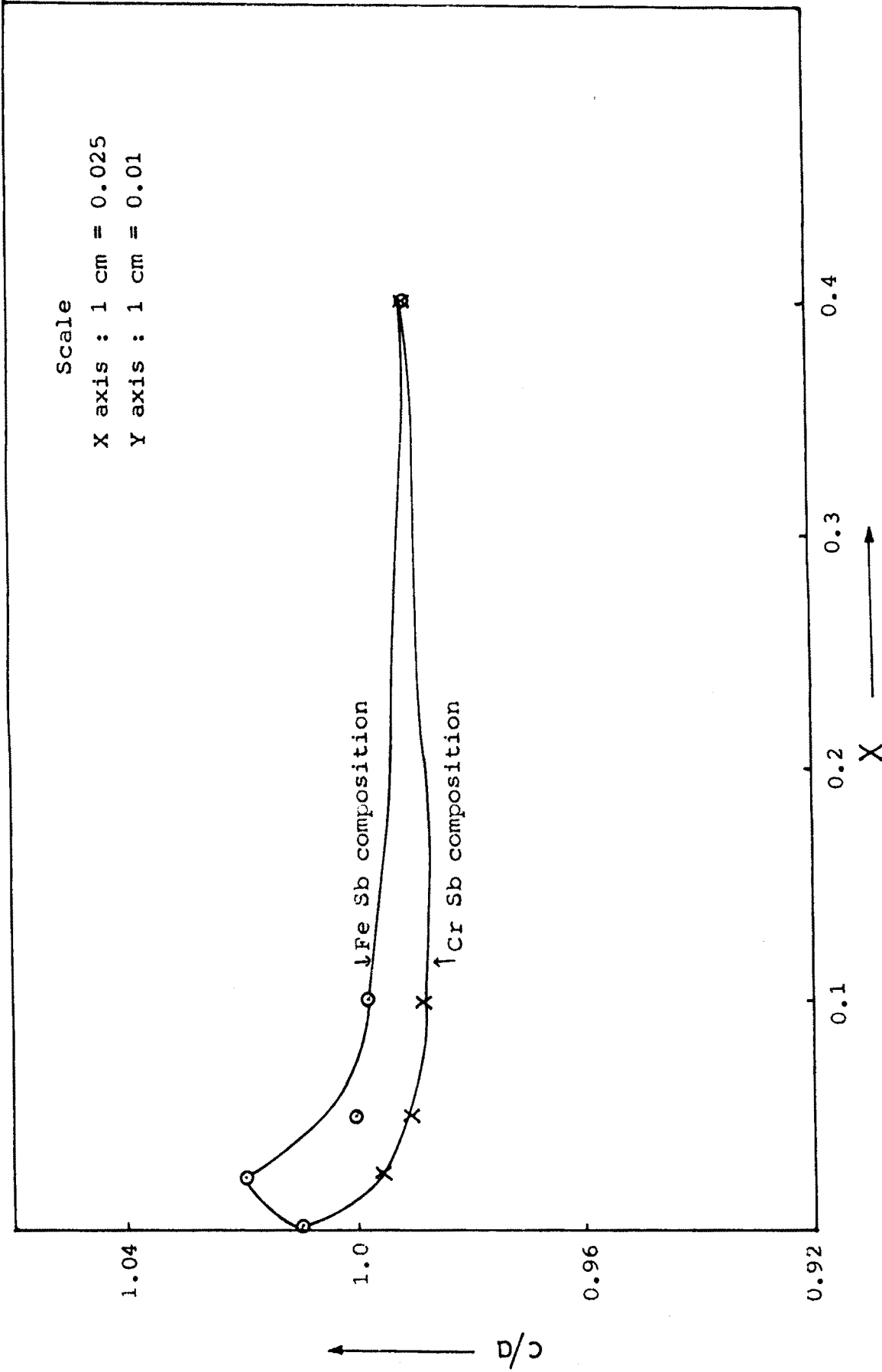


Fig. 3.10 : THE VARIATION OF c/a WITH x FOR BOTH SUBSTITUTIONS.

passes through a maximum for Fe Sb series with maximum at around $x = 0.025$ while for Cr Sb series the c/a passes through a broad minimum at $x = 0.1$. It is note worthy that the c/a is less than that observed for $BaTiO_3$ except for the compositions $Ba Fe_{x/2} Sb_{x/2} Ti_{1-x}O_3$ for $x = 0.025$.

These observations could be co-related to the variation of tolerance factor j with substitution. This parameter is given in table 2.1 and indicates a tendency of the material to become more and more cubic. The c/a approaching one as x increases is the indication of structure becoming increasingly cubic.

The data also suggests that the ferroelectric and electrical properties may show an interesting variation for substitutions below $x = 0.1$ and then a saturation may occur.

Further, the parameter a is observed to increase very slowly as x for Fe Sb series, while for Cr Sb series it doesnot vary significantly and systematically.

TABLE 3.1

Lattice Parameters For $\text{BaFe}_{x/2}\text{Sb}_{x/2}\text{Ti}_{(1-x)}\text{O}_3$

Concentration x	Lattice Parameters		c/a
	a \AA	c \AA	
0.00	3.9905	4.0304	1.01
0.025	3.96336	4.0426	1.02
0.05	3.9901	3.9901	1.00
0.1	4.00702	3.9900	0.99
0.2			
0.4	4.0210	3.9808	0.99

Table 3.2

Lattice Parameters For $\text{BaCr}_{x/2}\text{Sb}_{x/2}\text{Ti}_{(1-x)}\text{O}_3$

Concentration x	Lattice Parameters		c/a
	a \AA	c \AA	
0.025	4.0109	3.9948	0.996
0.05	4.0938	4.00529	0.99
0.1	4.0274	3.979	0.988
0.2			
0.4	4.0534	4.0129	0.99